Raman scattering in germanium-silicon alloys under hydrostatic pressure

Zhifeng Sui, Hubert H. Burke, and Irving P. Herman
Department of Applied Physics and the Microelectronics Sciences Laboratories, Columbia University, New York, New York 10027
(Received 16 February 1993)

The pressure dependence of vibrational Raman scattering in polycrystalline $Ge_{1-x}Si_x$ alloys is studied up to ~100 kbar across the compositional range, and the mode Grüneisen parameters γ for the Si-Si, Ge-Ge, and Ge-Si optical phonons are determined from the Raman shifts. $\gamma_{Si\text{-}Si}$ increases with the Ge fraction of the alloy and $\gamma_{Ge\text{-}Ge}$ increases with the Si fraction. The dependence of the Raman shift on x and pressure is described by a modified cellular isodisplacement model of optical phonons. In particular, the predicted dependence of the Ge-Si mode frequency on alloy composition at ambient pressure is found to agree much better with experiment when the variation of the average Ge-Si bond length with alloy composition is included in this model.

I. INTRODUCTION

Crystalline $Ge_{1-x}Si_x$ alloys have been the subject of recent intensive study due to their importance in new electronic and optical devices.[1,2] Raman scattering has been used to investigate the role of structural disorder on the vibrational and electronic properties of these alloys and the importance of strain in heterostructures composed of $Ge_{1-x}Si_x$, Si, and Ge.[1–11] However, the effect of strain on phonons in these alloys and heterostructures is still not well understood. To address this further, first-order Raman scattering has been performed on polycrystalline $Ge_{1-x}Si_x$ alloys that were subjected to hydrostatic pressure up to ~100 kbar in a diamond-anvil cell. The magnitude of strains in these experiments is of the same order as those in $Si/Ge_{1-x}Si_x/Ge$ heterostructures (0–4 %).

The optical phonon frequencies in $Ge_{1-x}Si_x$ decrease with temperature,[3] in part because of thermal expansion. This effect depends on the mode Grüneisen parameters $\gamma_i = -d\ln\omega_i/d\ln V$, where ω_i is the phonon frequency of mode i and V is the volume. However, different dependences of γ_i on alloy composition were found in the two previous studies of the Grüneisen parameters for these alloys.[4,5] One specific motivation for the current study is to resolve these differences and to examine a wider range of alloy compositions than has been studied previously.

The first-order Raman spectrum of $Ge_{1-x}Si_x$ has three dominant features, near 300, 400, and 500 cm^{-1} at ambient pressure, which are due to the optical-phonon modes associated with local Ge-Ge, Ge-Si, and Si-Si vibrations, respectively.[6–8] Some additional weak features between 400 and 500 cm^{-1}, due to Si-Si motion in the neighborhood of one or more Ge atoms, have been observed by Alonso and Winer.[9] Generally, the Si-Si (Ge-Ge) optical-phonon frequency decreases nearly linearly as the Ge (Si) concentration increases, while the frequency of the Ge-Si mode has a maximum near $x=0.5$.[7,8] Recently, the Ge-Ge mode frequency has been observed to increase with x for $x<0.02$, which is an exception to these trends.[10]

This dependence of phonon frequency on alloy composition can be attributed to the different effects of alloying in this mixed crystal. The Si/Ge mass difference affects the phonon density of states. The Si-Si (Ge-Ge) bonds are stretched (compressed) in crystalline $Ge_{1-x}Si_x$ relative to those in c-Si (c-Ge),[4] and the force constant of each bond is changed by this strain. This change causes a decrease (increase) in the Si-Si (Ge-Ge) phonon mode frequency, and also affects the Ge-Si mode frequency. Because the Si-Si, Ge-Si, and Ge-Ge bond lengths in c-Si, $Ge_{0.5}Si_{0.5}$, and c-Ge, respectively, are so different, there is structural disorder in the alloy. Therefore there is a distribution of Si-Si, Ge-Si, and Ge-Ge bond lengths about an average because of this disorder, which leads to inhomogeneity in the three local mode frequencies in the alloy and broadening of the three Raman peaks. Finally, while first-order Raman scattering in pure crystals is limited to $\mathbf{q}=\mathbf{0}$ phonons, the loss of translational symmetry that occurs with alloying relaxes this constraint. Because of this effect, the alloy Raman spectrum may resemble somewhat the density of states for optical phonons.

Renucci, Renucci, and Cardona[5] suggested that the Si-Si and Ge-Ge Raman peaks are due to phonons from the zone boundary, where the density of states has a maximum, rather than $\mathbf{q}=\mathbf{0}$ phonons. This was based on their measurements of γ_i for different alloy compositions. Lannin[11] compared the first-order spectrum of c-$Ge_{1-x}Si_x$ with the second-order Raman spectrum, which reflects the density of states of overtone transitions. In contrast to Ref. 5, he concluded that first-order spectra reflect mainly $\mathbf{q}=\mathbf{0}$ phonons, except at rather high alloy concentrations. Ishidate *et al.*[4] suggested that a bond charge of about 0.5 e in the alloy could be responsible for the decrease of the Si-Si and Ge-Ge frequencies; however, this suggested bond charge is much larger than is reasonable ($<0.1\ e$).[12,13]

Several calculations have sought to simulate the $Ge_{1-x}Si_x$ Raman spectrum. In varying degrees they have included the mass and force differences between Si and Ge, and the various effects of structural disorder. Calculations based on the coherent-potential approxima-

0163-1829/93/48(4)/2162(7)/$06.00

tion (CPA) (Ref. 14) account for the effects of mass defects and result in spectral density functions at $\mathbf{q}=0$ that simulate the x dependence of the Si-Si and Ge-Ge modes fairly well, but they do not account for the Ge-Si mode. The importance of local clustering in lattice dynamics was demonstrated in a calculation of the density of states for amorphous $Ge_{1-x}Si_x$,[15] which simulated all the major features of the Raman spectra observed in crystalline alloys. Zinger, Ipatova, and Subashiev[16] used the cellular isodisplacement (CI) model for $\mathbf{q}=\mathbf{0}$ phonons to fit the frequencies of the three main alloy peaks at ambient pressure. As presented in Ref. 16, this model accounts for differences of the Si and Ge masses and force constants, and simulates the Raman spectrum well across most of the composition range, except near $x=0$ and 1 for the Ge-Si mode. Alonso and Winer[9] relaxed a 216-atom supercell using the Keating potential and then diagonalized the dynamical matrix to obtain the first-order Raman spectrum. This procedure predicts the three stronger Raman features as well as the weaker ones, and demonstrates the importance of inhomogeneities due to strain relaxation and the local clustering of Si and Ge atoms. In the current study, the cellular isodisplacement model from Ref. 16 was modified and then used to study the three main Raman features both at ambient pressure and elevated pressure.

II. EXPERIMENTAL PROCEDURE AND RESULTS

Polycrystalline $Ge_{1-x}Si_x$ alloys, with an average grain size of 10–20 μm as determined by scanning electron microscopy, were grown by the horizontal Bridgeman technique, as detailed in Ref. 3. Pressure (p) was applied with a gasketed diamond-anvil cell. A 4:1 methanol-ethanol mixture solution was used to maintain nearly hydrostatic conditions, and the pressure was measured by the fluorescence from a small ruby chip placed near the sample.

Raman spectra were taken in backscattering geometry at room temperature using the 488-nm line from an Ar-ion laser. The scattered light was collected with a focusing lens and was directed into a triple monochromator. The dispersed light was detected by a cooled 1024-channel photodiode array; the overall spectral resolution was <0.6 cm^{-1}.

Figure 1 shows typical first-order Raman spectra of polycrystalline $Ge_{1-x}Si_x$ alloys at ambient pressure for different compositions. Figure 2 shows the dependence of the three Raman peak frequencies ω_i on pressure for a typical run (i=Si-Si, Ge-Si, Ge-Ge), where $\sim$20–30 spectra were collected for pressures up to $\sim$75–100 kbar. The linear coefficient $d\omega_i/dp$ for each mode was determined by fitting $\omega_i(p)$ with p and p^2 terms. The Raman linewidth remained essentially the same (within 1 cm^{-1}) for each mode throughout the pressure range examined.

Figure 3 presents the measured $d\omega_i/dp$ for the three modes. $d\omega_{\text{Si-Si}}/dp$ increases from 0.52 ± 0.03 cm^{-1}/kbar for c-Si ($x=1$) to 0.80 ± 0.03 cm^{-1}/kbar at $x=0.37$, while $d\omega_{\text{Ge-Ge}}/dp$ increases from 0.39 ± 0.02 cm^{-1}/kbar for c-Ge ($x=0$) to $\sim0.428\pm0.02$ cm^{-1}/kbar at $x=0.55$. $d\omega_{\text{Ge-Si}}/dp$ decreases from 0.58 ± 0.02 cm^{-1}/kbar at $x=0.11$ to 0.43 ± 0.02 cm^{-1}/kbar at $x=0.69$.

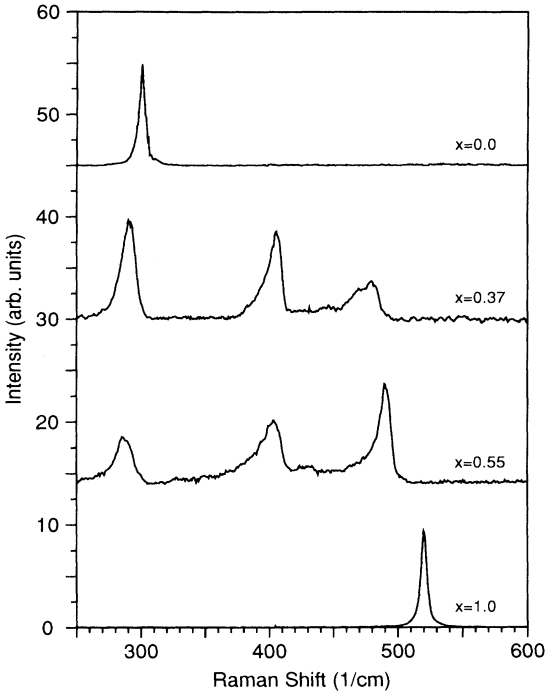

FIG. 1. The Raman spectra of c-Ge ($x=0.0$), $Ge_{1-x}Si_x$ with $x=0.37$ and 0.55, and c-Si ($x=1.0$) at ambient pressure and room temperature. The peaks near 500, 400, and 300 cm^{-1} correspond to the local Si-Si, Ge-Si, and Ge-Ge modes, respectively.

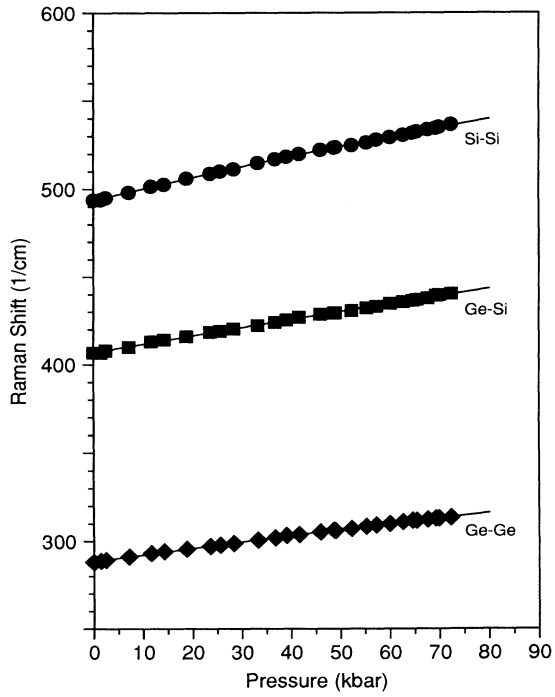

FIG. 2. Raman frequencies as a function of pressure for $Ge_{0.45}Si_{0.55}$. The solid lines are least-square fits including linear and quadratic terms in pressure.

III. THE ISODISPLACEMENT MODEL

The Hamiltonian of the lattice of a mixed crystal, including anharmonic terms, has the form

$$H=\tfrac{1}{2}\sum_{\alpha ls} m_{ls}[\dot{u}_\alpha(ls)]^2 + \tfrac{1}{2}\sum_{\alpha ls}\sum_{\beta l's'}\Phi_{\alpha\beta}\begin{bmatrix} l & l' \\ s & s' \end{bmatrix} u_\alpha(l,s)u_\beta(l',s') + \tfrac{1}{6}\sum_{\alpha ls}\sum_{\beta l's'}\sum_{\gamma l''s''}\Phi_{\alpha\beta\gamma}\begin{bmatrix} l & l' & l'' \\ s & s' & s'' \end{bmatrix} \times u_\alpha(l,s)u_\beta(l',s')u_\gamma(l'',s'') , \quad (1)$$

where $u_\alpha(l,s)$ is the αth component of the vector representing the displacement of the atom s from its equilibrium position in the unit cell l; m_{ls} is the mass of the (l,s) atom, and the coupling coefficients are

$$\Phi_{\alpha\beta}\begin{bmatrix} l & l' \\ s & s' \end{bmatrix} = \left[\frac{\partial^2\Phi}{\partial u_\alpha(l,s)\partial u_\beta(l',s')}\right]_0 , \quad (2)$$

$$\Phi_{\alpha\beta\gamma}\begin{bmatrix} l & l' & l'' \\ s & s' & s'' \end{bmatrix} = \left[\frac{\partial^3\Phi}{\partial u_\alpha(l,s)\partial u_\beta(l',s')\partial u_\gamma(l'',s'')}\right]_0 . \quad (3)$$

The displacement component $u_\alpha(l,s)$ is composed of two terms. The first describes a homogeneous deformation of the crystal, caused by external hydrostatic pressure or thermal expansion, and the second describes arbitrary displacements of the atoms from their new positions in the deformed crystal w_α:

$$u_\alpha(l,s)=\sum_\beta \varepsilon_{\alpha\beta}x_\beta(l,s)+w_\alpha(l,s) . \quad (4)$$

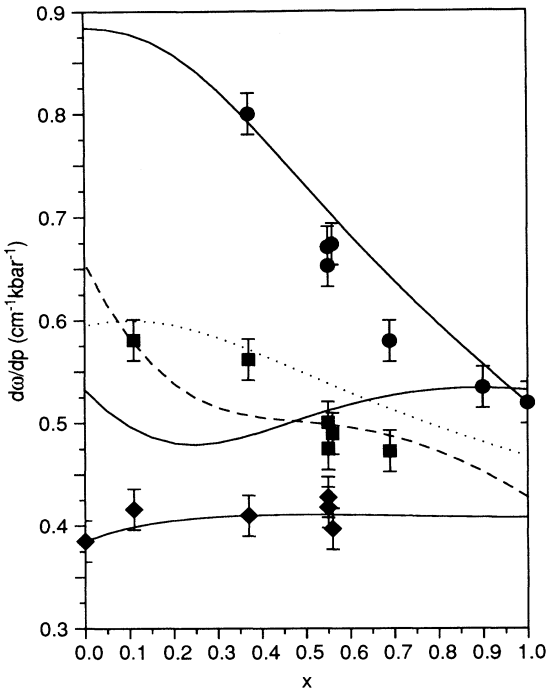

FIG. 3. $d\omega_i/dp$ as a function of the Si fraction x for the Si-Si (circles), Ge-Si (squares), and Ge-Ge (diamonds) modes. The solid lines are calculated by using the CI model with $dZ/dp=0$ for the Ge-Si mode. The dashed curve for the Ge-Si mode is a fit to the CI model with $dZ/dp=-180$ cm^{-2}/kbar, and the dotted curve for the Ge-Si mode is fit by using the simple model of Eq. (11).

The vector $\mathbf{x}(l,s)$ is the position vector of the (l,s) atom in the undeformed crystal. The parameters $\varepsilon_{\alpha\beta}$ are the elements of the deformation tensor, which are functions of hydrostatic pressure and temperature.

Substituting Eq. (4) into Eq. (1) gives

$$H=\tfrac{1}{2}\sum_{\alpha ls} m_{ls}[\dot{w}_\alpha(l,s)]^2+\tfrac{1}{2}\sum_{\alpha ls}\sum_{\beta l's'}\sum_{\mu\lambda}\Phi_{\alpha\beta}\begin{bmatrix} l & l' \\ s & s' \end{bmatrix}\varepsilon_{\alpha\mu}x_\mu(l,s)\varepsilon_{\beta\lambda}x_\lambda(l's') + \sum_{\alpha ls}\sum_{\beta l's'}\sum_{\mu}\Phi_{\alpha\beta}\begin{bmatrix} l & l' \\ s & s' \end{bmatrix}\varepsilon_{\alpha\mu}x_\mu(l,s)w_\beta(l',s')+\tfrac{1}{2}\sum_{\alpha ls}\sum_{\beta l's'}\Phi_{\alpha\beta}\begin{bmatrix} l & l' \\ s & s' \end{bmatrix}w_\alpha(l,s)w_\beta(l',s') + \tfrac{1}{2}\sum_{\alpha ls}\sum_{\beta l's}\sum_{\gamma l''s''}\sum_{\mu}\Phi_{\alpha\beta\gamma}\begin{bmatrix} l & l' & l'' \\ s & s' & s'' \end{bmatrix}w_\alpha(l,s)w_\beta(l',s')\varepsilon_{\gamma\mu}x_\mu(l'',s'')+O(\varepsilon^3)+O(w\varepsilon^2)+(Ow^3) . \quad (5)$$

The terms linear in $w_\beta(l',s')$ vanish because there is no net force when all the atoms are at their equilibrium positions in the homogeneously deformed crystal. The second term in Eq. (5) is the static energy, which does not contribute to the dynamics.

After excluding the static contributions and higher-order terms, the Hamiltonian can be rewritten as

$$H'=\tfrac{1}{2}\sum_{\alpha ls} m_{ls}[\dot{w}_\alpha(l,s)]^2 + \tfrac{1}{2}\sum_{\alpha ls}\sum_{\beta l's'}\Omega_{\alpha\beta}\begin{bmatrix} l & l' \\ s & s' \end{bmatrix}w_\alpha(l,s)w_\beta(l',s') , \quad (6)$$

where

$$\Omega_{\alpha\beta}\begin{bmatrix} l & l' \\ s & s' \end{bmatrix} = \Phi_{\alpha\beta}\begin{bmatrix} l & l' \\ s & s' \end{bmatrix} + \sum_{\gamma l'' s''}\sum_{\mu}\Phi_{\alpha\beta\gamma}\begin{bmatrix} l & l' & l'' \\ s & s' & s'' \end{bmatrix}\varepsilon_{\gamma\mu}x_{\mu}(l'',s'') \ . \tag{7}$$

This Hamiltonian is quasiharmonic. Hydrostatic pressure affects the force constants through the anharmonic contributions in Eq. (7), and the changes in strain $\varepsilon_{\gamma\mu}$ are usually proportional to p in the low-pressure limit.

If $\Phi_{\alpha\beta}$ and $\Phi_{\alpha\beta\gamma}$ were known, then Eq. (6) would give a good description of the system; however, the calculation would still be very complex. Several simplifying assumptions lead to the cellular isodisplacement (CI) approximation, as applied to $Ge_{1-x}Si_x$ at ambient pressure by Zinger, Ipatova, and Subashiev,[16] which involves only a few parameters to be determined by experiment. This model assumes the following. (i) There are only harmonic contributions to the Hamiltonian. (ii) There are three distinguishable types of cells or clusters of two atoms: Si-Si, Ge-Si, and Ge-Ge. (iii) The Hamiltonian is expressed in terms of the centers of gravity of the cells and the relative displacements of the atoms in the cells of the same kind, with intercell and intracell interactions treated as model parameters. (iv) Configurational ensemble averages of the Hamiltonian are made, which are expressed in terms of x. (v) Only long-wavelength vibrations in an isotropic medium are considered. This simplifies the Hamiltonian and leads to six independent equations of motion corresponding to three acoustic models and three optical modes. (vi) Acoustic modes are ignored, and the coupling of acoustic and optics modes is neglected since the intracell force constants far exceed those for intercell interactions.

Then the three long-wavelength optical-mode frequencies $\omega=\omega_i$ are determined by[16]

$$\begin{vmatrix} \omega^2-\omega_2^2+x(2-x)T & -x^2A_1 & -2x(1-x)A_3 \\ -(1-x)^2A_2 & \omega^2-\omega_1^2+(1-x^2)S & -2x(1-x)A_5 \\ -(1-x)^2A_4 & -x^2A_6 & \omega^2-\omega_3^2+\dfrac{(1-2x)^2}{2}W \end{vmatrix} = 0 \ , \tag{8}$$

where ω_1 and ω_2 correspond to the phonon frequencies of c-Si and c-Ge, respectively, and ω_3 is approximately $\omega_{\text{Ge-Si}}$ for $Ge_{0.5}Si_{0.5}$. These three parameters are set equal to 520.5, 301.3, and 406.0 cm^{-1}, respectively (ambient pressure, $\varepsilon_{\gamma\mu}=0$). The other three independent parameters T, S and W describe intercell interactions, which are related to A_1-A_6 by[16]

$$A_1=\tfrac{1}{2}\left[T+\frac{m_{\text{Si}}}{m_{\text{Ge}}}S\right]=\frac{m_{\text{Si}}}{m_{\text{Ge}}}A_2 \ , \tag{9a}$$

$$A_3=\tfrac{1}{2}\left[T+\frac{2\mu}{m_{\text{Ge}}}W\right]=\frac{2\mu}{m_{\text{Ge}}}A_4 \ , \tag{9b}$$

$$A_5=\tfrac{1}{2}\left[S+\frac{2\mu}{m_{\text{Si}}}W\right]=\frac{2\mu}{m_{\text{Si}}}A_6 \ , \tag{9c}$$

where $\mu=m_{\text{Si}}m_{\text{Ge}}/(m_{\text{Si}}+m_{\text{Ge}})$ is the reduced mass of the Ge-Si cell.

In the limit of $x=0$, the solutions of Eq. (8) are $\omega^2_{\text{Si-Si}}(0)=\omega_1^2-S$, $\omega_{\text{Ge-Ge}}(0)=\omega_2$, and $\omega^2_{\text{Ge-Si}}(0)=\omega_3^2-W/2$, while in the limit of $x=1$, the solutions are $\omega_{\text{Si-Si}}(1)=\omega_1$, $\omega^2_{\text{Ge-Ge}}(1)=\omega_2^2-T$, and $\omega^2_{\text{Ge-Si}}(1)=\omega_3^2-W/2$. Zinger, Ipatova, and Subashiev fit the observed dependence of $\omega_{\text{Si-Si}}$ and $\omega_{\text{Ge-Ge}}$ on x by setting $T=0.11\omega_2^2$, $S=0.20\omega_1^2$, and $W=(T+S)/2$, which gives $\omega_{\text{Ge-Si}}(x=0)=\omega_{\text{Ge-Si}}(x=1)=387$ cm^{-1}. However, experimentally $\omega_{\text{Ge-Si}}(0)=387$ cm^{-1}, while $\omega_{\text{Ge-Si}}(1)=400$ cm^{-1}.

This asymmetry could be due to the different Ge-Si bond lengths at the two composition limits. As pointed out in Refs. 10 and 17, the average Ge-Si bond length (r) is $\sim 1\%$ larger in the Ge-rich alloy ($x\sim 0$) than in the Si-rich alloy ($x\sim 1$). With $\Delta\omega_{\text{Ge-Si}}=-3\gamma_{\text{Ge-Si}}\omega_{\text{Ge-Si}}(\Delta r/r)$ and $\gamma_{\text{Ge-Si}}=1.3$, which is extrapolated from the data presented here, $\omega_{\text{Ge-Si}}$ would be expected to be ~ 15 cm^{-1} higher in the Si-rich region than in the Ge-rich region. This agrees with experiment. To include this effect in the CI model, the term $(0.5-x)Z=6\gamma_{\text{Ge-Si}}\omega^2_{\text{Ge-Si}}(0.5-x)/100$ is added to the third diagonal element in the determinant of Eq. (8). This assumes a linear variation of the average bond length from the Ge- to Si-rich alloy, with $\Delta r/r=(0.5-x)/100$, as was suggested by Refs. 10 and 17. Because the variation of $\gamma_{\text{Ge-Si}}$ and $\omega_{\text{Ge-Si}}$ with x is relatively small, Z is determined by using data for $x\sim 0.5$.

Similarly, since the average Si-Si and Ge-Ge bond lengths in the alloy depend on x,[10,17] these bond-length variations will also affect these modes. However, it was found that a similar modification to Eq. (8) gave almost the same compositional dependence of the Raman frequencies, though with different S and T. This strain-modified CI model deviated from the original fit only slightly when $x<0.2$ for the Si-Si mode and $x>0.7$ for the Ge-Ge mode. Therefore, over most of the compositional range the corrections due to Si-Si and Ge-Ge bond stretching and compression can be included within the parameters S and T, and the strain-modified CI model explicitly includes only the effect of composition-dependent Ge-Si bond lengths.

Figure 4 plots ω_i vs x from Refs. 7 and 8, along with fits using the original CI model (solid lines) for the three modes and the CI model modified for Ge-Si bond-length variations (dashed line). All model parameters are listed

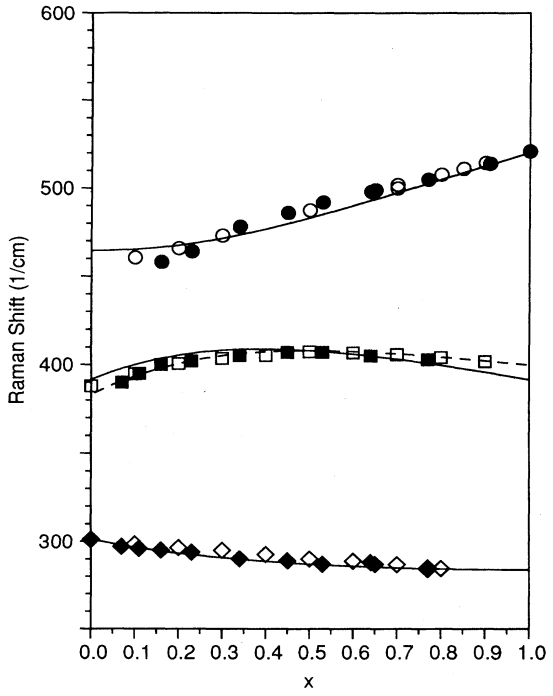

FIG. 4. The Raman frequencies ω_i vs Si fraction x, showing the Si-Si (circles), Ge-Si (squares), and Ge-Ge (diamonds) modes. The experimental data are taken from Ref. 7 (solid symbols) and Ref. 8 (open symbols). The solid curves are fits using the original CI model. The dashed curve for the Ge-Si mode uses the CI model modified for average bond-length variations.

in Table I. The original model describes the Si-Si and Ge-Ge modes quite well. Including the effect of local strain clearly improves the description of the Ge-Si mode.

The quasiharmonic form of the Hamiltonian [Eqs. (6) and (7)] is used to model $d\omega_i(x)/dp$ (Fig. 3), once again by employing the CI approximation. Hydrostatic pressure changes the force constants in Eq. (7) because of anharmonic effects. To first order, this causes the six parameters in the original CI model ω_1, ω_2, ω_3, T, S, and W to vary linearly with p, such as $\omega_1(p)=\omega_1+(d\omega_1/dp)p$, and leads to six new parameters $d\omega_1/dp$, etc. $d\omega_i/dp$ for the three modes are obtained as a function of composition by taking the derivative of Eq. (8) with respect to p. $d\omega_1/dp$ and $d\omega_2/dp$ are set equal to 0.52 cm^{-1}/kbar (Ref. 18) and 0.385 cm^{-1}/kbar,[19] the values for c-Si and c-Ge, respectively. $d\omega_3/dp$ is taken to be 0.44 cm^{-1}/kbar. The other three pressure derivatives are treated as model parameters to be determined by the experimental data. Fits of $d\omega_i/dp$ with this modified CI model are shown in Fig. 3.

TABLE I. The parameters in the CI model.

ω_1 (cm^{-1})	521	$d\omega_1/dp$ (cm^{-1}/kbar)	0.52
ω_2 (cm^{-1})	301	$d\omega_2/dp$ (cm^{-1}/kbar)	0.385
ω_3 (cm^{-1})	412	$d\omega_3/dp$ (cm^{-1}/kbar)	0.44
S (cm^{-2})	0.20 ω_1^2	dS/dp (cm^{-2}/kbar	−280
T (cm^{-2})	0.11 ω_2^2	dT/dp (cm^{-2}/kbar)	0.0
Z (cm^{-2})	0.078 ω_3^2	dZ/dp (cm^{-2}/kbar)	0.0, −180

$d\omega_{\text{Si-Si}}/dp$ is sensitive to dS/dp, and the curve for the Si-Si mode in Fig. 3 is best fit with $dS/dp=-280$ cm^{-2}/kbar. In the Ge-rich regime ($x\to 0$), $d\omega_{\text{Si-Si}}/dp\to 0.88$ cm^{-1}/kbar. This is roughly equal to $d\omega_{\text{Si-Si}}/dp$ in amorphous Si, which is 1.0±0.3 cm^{-1}/kbar,[20] suggesting that structural disorder is similar in both materials.

The Ge-Ge mode is sensitive to dT/dp, and the curve for the Ge-Ge mode in Fig. 3 is fit with $dT/dp=0$. In the Si-rich region ($x\to 1$), $d\omega_{\text{Ge-Ge}}/dp\to 0.42$ cm^{-1}/kbar. Lannin[11] suggested that the slower dependence of $\omega_{\text{Ge-Ge}}$ with composition relative to that for $\omega_{\text{Si-Si}}$ means that the Ge-Ge mode is more extended than the Si-Si mode. Similarly $d\omega_{\text{Ge-Ge}}/dp$ varies with composition much slower than does $d\omega_{\text{Si-Si}}/dp$, which may reinforce this conclusion. The CI model accounts for these differences between the Si-Si and Ge-Ge modes.

For the Ge-Si mode, the pressure derivative of the third diagonal element in Eq. (8), modified for local strain, gives $2\omega(d\omega/dp)-2\omega_3(d\omega_3/dp)+[(1-2x)^2/2]dW/dp+(0.5-x)dZ/dp$, where $dW/dp=(dT/dp+dS/dp)/2$. Ignoring the strain term, which is the last term, gives the solid curve for $d\omega_{\text{Ge-Si}}/dp$ in Fig. 3. The fit is not very good.

Two factors in Z, which describes the effect of the variation of average bond length with x, depend on pressure: $\omega_{\text{Ge-Si}}$ and $\Delta r/r$. $\omega^2_{\text{Ge-Si}}(p)$ increases with pressure as $\omega^2_{\text{Ge-Si}}(1\text{ bar})[1+2p\gamma_{\text{Ge-Si}}(x)/3B(x)]$, where B is the bulk modulus. Because $B_{\text{Si}}>B_{\text{Ge}}$, the difference in Si-Si and Ge-Ge bond lengths in c-Si and c-Ge decreases with pressure. At low pressures, this decrease is linear with p. So $\Delta r/r\propto(1-p/p_c)$, where $p_c\sim 330$ kbar. ($\Delta r/r$ never reaches 0 because the pressure/volume equation of state is nonlinear and because of phase transitions.) Since $B(x=0.5)\sim 850$ kbar, these two effects partially cancel, and this dZ/dp term does not affect the Ge-Si curve in Fig. 3 very much. Treating dZ/dp as a free parameter gives the dashed Ge-Si curve in Fig. 3 with $dZ/dp=-180$ cm^{-2}/kbar. However, this value is much too large to be accounted for by strain.

Though the modified CI model fits $d\omega_{\text{Si-Si}}/dp$ and $d\omega_{\text{Ge-Ge}}/dp$ well (Fig. 3), the $d\omega_{\text{Ge-Si}}/dp$ fit is poor, perhaps because of the assumption connecting W with S and T. A better fit is obtained for the Ge-Si mode using the following simple model. If only intracell interactions are considered, with the same force constant k for the three local vibrations, then $\omega_{\text{Si-Si}}=\sqrt{2k/m_{\text{Si}}}$, $\omega_{\text{Ge-Ge}}=\sqrt{2k/m_{\text{Ge}}}$, and $\omega_{\text{Ge-Si}}=\sqrt{k/\mu}$. They are related by

$$\omega^2_{\text{Ge-Si}}=\alpha\omega_{\text{Si-Si}}\omega_{\text{Ge-Ge}}\ , \tag{10}$$

where $\alpha=(m_{\text{Si}}+m_{\text{Ge}})/2\sqrt{m_{\text{Si}}m_{\text{Ge}}}=1.11$. If it is assumed that Eq. (10) is still valid when $\omega_{\text{Si-Si}}(x)$ and $\omega_{\text{Ge-Ge}}(x)$ are used from the CI model, then $\gamma_{\text{Ge-Si}}(x)$ is obtained. The fit to the data in Fig. 4 is fairly good but not as good as the original and modified CI models. In particular, this simple model does not reproduce the

downward curvature in the CI model fits. Now, differentiating Eq. (10) with respect to p leads to

$$\frac{d\omega_{\text{Ge-Si}}(x)}{dp}=\frac{\alpha}{2}\left[\left[\frac{\omega_{\text{Ge-Ge}}(x)}{\omega_{\text{Si-Si}}(x)}\right]^{1/2}\frac{d\omega_{\text{Si-Si}}(x)}{dp}+\left[\frac{\omega_{\text{Si-Si}}(x)}{\omega_{\text{Ge-Ge}}(x)}\right]^{1/2}\frac{d\omega_{\text{Ge-Ge}}(x)}{dp}\right]. \quad (11)$$

This is plotted as the dotted line in Fig. 3 by using $d\omega_{\text{Si-Si}}(x)/dp$ and $d\omega_{\text{Ge-Ge}}(x)/dp$ from the CI model. This fit of $d\omega_{\text{Ge-Si}}(x)/dp$ is good, and is better than that directly from the CI model.

IV. DISCUSSION

The mode Grüneisen parameter $\gamma_i=-d\ln\omega_i/d\ln V_{V\to V(1\text{ bar})}=[B(x)/\omega_i](d\omega_i/dp)_{p\to 1\text{ bar}}$, where V is the volume. Though both relations should give the same γ_i, use of the pressure relation is usually less precise because of the nonlinear relation of p and V. The $\omega_i(p)$ data are converted to $\omega_i(V)$ by using Murnaghan's equation of state,[18]

$$\frac{\Delta V}{V}=\left[1+\frac{B'(x)}{B(x)}p\right]^{1/B'(x)}-1, \quad (12)$$

where $\Delta V=V(p)-V(1\text{ bar})$ and $B'(x)=dB(x)/dp$. γ_i is determined by a least-squares linear fit of ω_i vs $\Delta V/V$.

This procedure is sensitive to the dependence of B and B' on x; unfortunately, there are limited experimental data describing this dependence. The bulk moduli of $Ge_{0.2}Si_{0.8}$, as determined by the thermoelastic stress,[21] and $Ge_{0.51}Si_{0.49}$, as determined by Brillouin scattering,[22] seem to obey Vegard's law of linear interpolation between B_{Si} and B_{Ge}. Reference 23, however, reported a bulk modulus for a polycrystalline $Ge_{1-x}Si_x$ alloy ($x=0.28,0.54,0.64$) that is much higher than expected by linear interpolation. $B'(x)$ has been reported to obey Vegard's law with only a slight deviation.[24] Linear interpolation of the bulk modulus $B(x)$ and $B'(x)$ between the values for c-Ge [$B=751$ kbar and $B'=4.75$ (Ref. 19)] and those for c-Si [$B=979$ kbar and $B'=4.2$ (Ref. 19)] is assumed here. The resulting mode Grüneisen parameters are plotted in Fig. 5.

Figures 3 and 5 show that $d\omega_{\text{Si-Si}}/dp$ and $\gamma_{\text{Si-Si}}$ both increase with Ge fraction. $d\omega_{\text{Ge-Ge}}/dp$ shows perhaps a weak increase with Si fraction x, but $\gamma_{\text{Ge-Ge}}$ shows a definite increase with x because of the dependence of B on x. $d\omega_{\text{Ge-Si}}/dp$ definitely decreases with x, but $\gamma_{\text{Ge-Si}}$ seems to reach a minimum near $x=0.5$.

The change of γ_i with composition for each mode is similar to that obtained in Ref. 5, where Grüneisen parameters were measured only up to 8 kbar and over a narrower compositional range. However, the current results differ with those in Ref. 4, where $d\omega_{\text{Ge-Ge}}/dp$ was found to decrease strongly with increasing x. This is definitely not seen here. Reference 4 examined polycrystalline films made by annealing amorphous films, whereas Ref. 5 and this study examined bulk polycrystalline alloys. However, this difference in sample preparation is not expected to be significant. In Ref. 4 measurements at only approximately four pressures were used to determine $d\omega_i/dp$ (including $p=1$ bar), in contrast to $\sim$20–30 different pressure measurements per run here. It is quite possible that there is significant error in the determination of $d\omega_i/dp$ in Ref. 4.

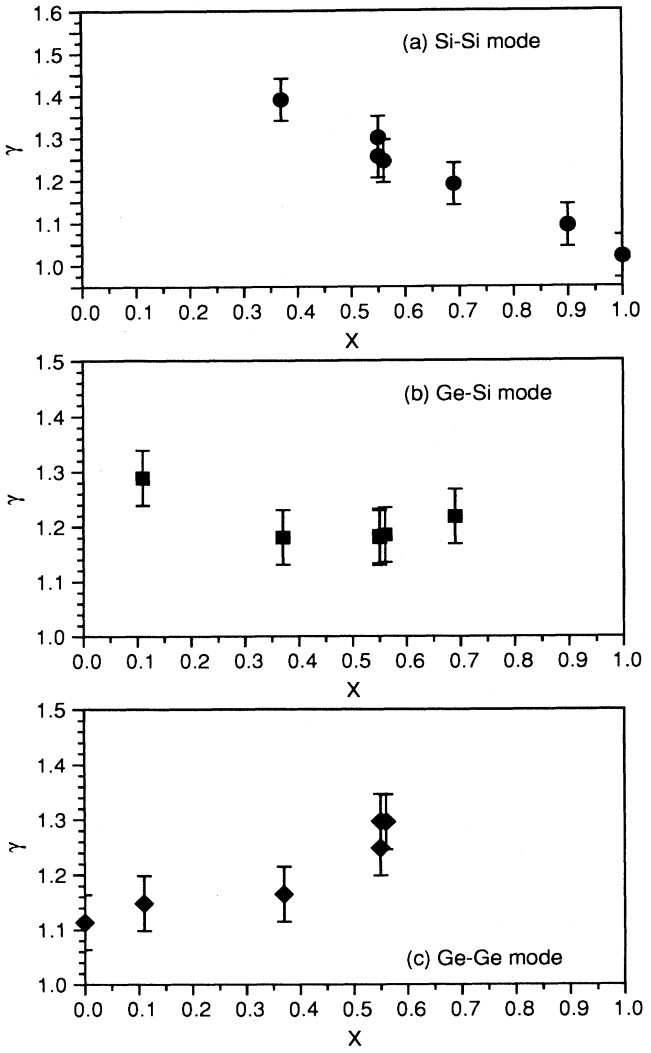

FIG. 5. The Grüneisen parameters γ_i as a function of the Si fraction x for the three modes.

Because of the relaxation of momentum conservation in this disordered alloy, phonons with a range of "wave vectors" could be involved in first-order Raman scattering. Renucci, Renucci, and Cardona[5] argued that the increase of $\gamma_{\text{Si-Si}}$ ($\gamma_{\text{Ge-Ge}}$) with Ge (Si) fraction indicates that zone-boundary phonons, where the density of states is large, are important because γ is usually larger at the zone boundaries than at the zone center in c-Si (c-Ge). This conclusion was apparently negated by the second-order Raman study by Lannin.[11] Still, it is possible that further insight could be gained by analyzing the expected

dependence of the Raman linewidth on p.

Consider the Si-Si mode. In c-Si, $\omega_{LO,TO}$ is 521 cm^{-1} at Γ and decreases to 411 cm^{-1} at X and 420 cm^{-1} at L for the LO mode, and to 463 cm^{-1} at X and 493 cm^{-1} at L for the TO mode.[25] Based on measurements[18] and *ab initio* calculations[26] for c-Si, $\gamma_{LO,TO}$ is 0.98 at Γ, decreases to 0.82 at X, and increases to 1.3 at L for the LO mode, and increases to 1.5 at X and 1.3 at L for the TO mode. Because the examined samples are polycrystalline, it is not clear which branches are most important in Raman backscattering. (Unlike c-Si, the polarized and depolarized Raman spectra of these polycrystalline alloys are the same.) If TO phonons with a range of wave vectors along Σ or Δ, or LO phonons along Δ were most important, the Si-Si mode would narrow with increasing pressure, while if LO phonons along Σ were important, the Si-Si peak would broaden with p. (Such a broadening would have been experimentally observable for $p > 20$ kbar. However, such an observation would also imply that $\gamma_{Si\text{-}Si}$ decreases with Ge fraction, which would contradict the results presented in Fig. 5.) Since neither a narrowing nor a broadening is seen here for the Si-Si mode (or the other two modes), no definitive conclusions can be drawn.

V. CONCLUDING REMARKS

The Raman spectra of polycrystalline $Ge_{1-x}Si_x$ alloys were measured across much of the compositional range for hydrostatic pressures up to ~ 100 kbar. There is a clear linear increase in $\gamma_{Si\text{-}Si}$ with Ge content and of $\gamma_{Ge\text{-}Ge}$ with Si content. The dependence of $\omega_{Si\text{-}Si}$ and $\omega_{Ge\text{-}Ge}$ on alloy concentration and pressure can be successfully modeled with the cellular isodisplacement model. $\omega_{Ge\text{-}Si}(x)$ at ambient pressure is very well fit by the CI model when the variation of the average Ge-Si bond length with x is included. $\gamma_{Ge\text{-}Si}$ has a quadratic dependence on x, with a minimum near $x = 0.5$. The general decrease of $d\omega_{Ge\text{-}Si}/dp$ with x is moderately well fit by using the CI model predictions for the Si-Si and Ge-Ge modes. The determination of γ_i from experiments is sensitive to the dependence of the bulk modulus and its pressure derivative on alloy concentration.

ACKNOWLEDGMENTS

This work was supported at Columbia by the Joint Services Electronics Program Contract No. DAAL03-91-C-0016 and by the Office of Naval Research.

[1]T. P. Pearsall, Crit. Rev. Solid State Mater. Sci. **15**, 551 (1989).
[2]R. People and S. A. Jackson, Phys. Rev. B **36**, 1310 (1987).
[3]H. H. Burke and I. P. Herman (unpublished).
[4]T. Ishidate, S. Katagiri, K. Inoue, M. Shibuya, K. Tsuji, and S. Minomura, J. Phys. Soc. Jpn. **53**, 2584 (1984).
[5]J. B. Renucci, M. A. Renucci, and M. Cardona, Solid State Commun. **9**, 1651 (1971).
[6]D. W. Feldman, M. Ashkin, and J. H. Parker, Jr., Phys. Rev. Lett. **17**, 1209 (1966).
[7]J. B. Renucci, M. A. Renucci, and M. Cardona, *Proceedings of the Second International Conference on Light Scattering in Solids*, edited by M. Balkanski (Flammarion, Paris, 1971), p. 32.
[8]W. J. Brya, Solid State Commun. **12**, 253 (1973).
[9]M. I. Alonso and K. Winer, Phys. Rev. B **39**, 10056 (1989).
[10]H. D. Fuch, C. H. Grein, M. I. Alonso, and M. Cardona, Phys. Rev. B **44**, 13 120 (1991).
[11]J. S. Lannin, Phys. Rev. B **16**, 1510 (1977).
[12]W. A. Harrison, *Electronic Structure and Properties of Solids* (Freeman, San Francisco, 1980).
[13]A. Qteish and R. Resta, Phys. Rev. B **37**, 1308 (1988).
[14]V. Srivastava and S. K. Joshi, Phys. Rev. B **8**, 4671 (1973).
[15]F. Yndurain, Phys. Rev. Lett. **37**, 1062 (1976).
[16]G. M. Zinger, I. P. Ipatova, and A. V. Subashiev, Fiz. Tekh. Poluprovodn. **11**, 656 (1977) [Sov. Phys. Semicond. **11**, 383 (1977)].
[17]S. de Gironcoli, P. Giannozzi, and S. Baroni, Phys. Rev. Lett. **66**, 2116 (1991).
[18]B. A. Weinstein and G. J. Peirmarini, Phys. Rev. B **12**, 1172 (1975).
[19]D. Olego and M. Cardona, Phys. Rev. B **25**, 1151 (1981).
[20]T. Ishidate, K. Inoue, K. Tsuji, and S. Minomura, Solid State Commun. **42**, 197 (1982).
[21]W. B. Gauster, J. Appl. Phys. **44**, 1089 (1973).
[22]M. Mendik, M. Ospelt, H. von Känel, and P. Wachter, Appl. Surf. Sci. **50**, 303 (1991).
[23]V. T. Bublik, S. S. Gorelik, A. A. Zaitsev, and A. Y. Polyakov, Phys. Status Solidi B **66**, 427 (1974).
[24]G. Queisser and W. B. Holzapfel, Appl. Phys. A **53**, 114 (1991).
[25]G. Dolling, *Inelastic Scattering of Neutrons in Solids and Liquids* (IAEA, Vienna, 1963), Vol. II, p. 37.
[26]P. Giannozzi, S. de Gironcoli, P. Pavone, and S. Baroni, Phys. Rev. B **43**, 7231 (1991).